Multifunctional flame-retardant polycaprolactone interlayers for carbon riber-reinforced epoxy resin composites: Thermal degradation, fire behavior, and mechanical performance

Balogh F., Varga L. J., Marton G. Zs., Szebényi G., Toldy A.

Accepted for publication in Journal of Vinyl & Additive Technology
Published in 2026
DOI: 10.1002/vnl.70126

Check for updates

Journal of Vinyl and Additive Technology

SPECIAL ISSUE Current Trends in Polymer Degradation and Stabilization in Honor of Professor Norman S. Allen

WILEY | spe INSPIRING PLASTICS PROFESSIONALS

RESEARCH ARTICLE OPEN ACCESS

Multifunctional Flame-Retardant Polycaprolactone Interlayers for Carbon Fiber-Reinforced Epoxy Resin Composites: Thermal Degradation, Fire Behavior, and Mechanical Performance

Fanni Balogh[1,2] | László József Varga[1] | Gergő Zsolt Marton[1,2] | Gábor Szebényi[1,2] | Andrea Toldy[1,2]

[1]Department of Polymer Engineering, Faculty of Mechanical Engineering, Budapest University of Technology and Economics, Budapest, Hungary | [2]MTA-BME Lendület Sustainable Polymers Research Group, Budapest University of Technology and Economics, Budapest, Hungary

Correspondence: Andrea Toldy (atoldy@edu.bme.hu)

Received: 28 January 2026 | **Revised:** 2 June 2026 | **Accepted:** 4 June 2026

Keywords: additive manufacturing | flame retardancy | flame-retardant filament | interlayer | multifunctional layer | polycaprolactone (PCL) | polymer composites

ABSTRACT

Reducing flammability and controlling damage processes are critical challenges in carbon fiber-reinforced epoxy matrix polymer composites. The aim of the present study was to develop flame-retardant polycaprolactone (PCL) filaments and to apply them as additively manufactured interlayers in laminated composite systems. The research builds on a previously validated PCL-based solution that enables the control and localisation of mechanical damage. The novelty of the work lies in the multifunctionalisation of the interlayer, achieved by incorporating flame-retardant additives into the PCL, allowing the layer to simultaneously fulfill mechanical stabilization and fire-protection functions. The results demonstrate that PCL filaments modified with appropriately selected additives are compatible with additive manufacturing processes and, when applied as interlayers, favorably influence the fire response of composite laminates. The developed multifunctional layer may contribute to the advancement of intelligent, multifunctional polymer composite systems, as the introduction of a single interlayer enables the mitigation of different damage mechanisms.

1 | Introduction

The development of polymer composites represents one of the most dynamically advancing fields in materials science. In particular, carbon fiber-reinforced polymer (CFRP) systems have become dominant across numerous industrial sectors, including the automotive, aerospace, construction, and energy industries. Their widespread adoption is primarily attributed to their favorable specific mechanical properties, as they provide high stiffness and strength at relatively low weight. By combining different constituents, composite structures can achieve performance exceeding that of individual components. In parallel with the expansion of application areas, the performance requirements imposed on composite structures have become increasingly complex. Beyond conventional mechanical considerations, growing emphasis is placed on fire safety, controllability of damage evolution, and reliable, predictable failure behavior. A major drawback of fiber-reinforced polymer composites is that, under fire exposure, the polymer matrix is combustible and may generate heat and smoke, accompanied by the release of toxic combustion products [1, 2]. Addressing these challenges is, particularly, critical in structural applications where material behavior directly affects operational safety [3].

Failure in composite structures typically does not result from a single damage mechanism, but rather from a combination of

This is an open access article under the terms of the Creative Commons Attribution-NonCommercial-NoDerivs License, which permits use and distribution in any medium, provided the original work is properly cited, the use is non-commercial and no modifications or adaptations are made.

© 2026 The Author(s). Journal of Vinyl & Additive Technology published by Wiley Periodicals LLC on behalf of Society of Plastics Engineers.

Highlights

- Flame-retardant PCL filaments produced by fused filament fabrication.
- Expandable graphite raises PCL crystallization peak by ~17°C.
- pHRR reduced by ~25% in EG-modified PCL matrix specimens.
- EG-based interlayers improve the fire behavior of CFRP laminates.
- Flame-retardant additives improve PCL processability and interlayer placement.

multiple processes occurring either simultaneously or sequentially. The most common mechanisms include fiber fracture, matrix cracking, fiber pull-out caused by insufficient fiber–matrix interfacial adhesion, and interlaminar delamination [4]. The sequence and spatial distribution of these damage mechanisms fundamentally determine the energy absorption capacity, residual integrity, and likelihood of catastrophic failure of the structure. The modification and localization of failure constitute an advanced material and structural design strategy aimed at promoting more favorable damage mechanisms and spatially constraining damage development [4]. One of the most effective approaches to achieving this goal is targeted modification of interlaminar properties, for instance, through the incorporation of interlayer materials. Interlayers can slow crack propagation, localize damage, and enhance the energy absorption capability of the structure, while largely preserving the favorable mechanical properties of the load-bearing plies [5]. Numerous studies in the literature demonstrate that the introduction of thermoplastic interlayers can transform the typically sudden and catastrophic failure of composites into a more gradual, pseudo-ductile response [6]. Such systems offer the advantage that damage evolves in multiple stages, allowing warning signs to appear prior to final failure, which is of particular importance from a safety engineering perspective. Furthermore, damage often becomes localized along the interlayer, potentially facilitating repairability and extending service life [6].

Among thermoplastic polymers, polycaprolactone (PCL) has emerged as a particularly promising interlayer material. PCL is a biodegradable, semicrystalline polyester characterized by a low melting temperature, high deformability, and significant elongation at break [7–10]. These properties make it well-suited to function as a flexible, energy-absorbing phase in brittle epoxy matrix composites. Several studies have confirmed that the incorporation of PCL into epoxy-based systems can significantly improve toughness and impact resistance, while the reduction in strength remains moderate [11]. Previous investigations have also shown that, when applied as an interlayer material, PCL enables the design of both the location and progression of failure. By employing additive manufacturing technologies, PCL can be deposited locally onto composite plies in predefined geometries, thereby creating controlled crack-initiation zones [12–14]. The presence of an interlaminar PCL layer can promote stable crack propagation, increased toughness, and pseudo-ductile behavior, while global stiffness and strength characteristics are only marginally affected [12, 13].

However, as PCL exhibits limited thermal stability on its own, incorporating flame retardants is essential to ensure fire safety, especially in structural applications [15]. Current flame-retardant strategies extend beyond merely reducing material flammability and increasingly focus on slowing fire spread and maintaining structural integrity for as long as possible during fire exposure [1]. Conventional additive-based approaches often adversely affect mechanical performance or processability; consequently, increasing attention is being directed toward integrated, multifunctional solutions in which structural and fire safety functions are realized simultaneously [16–18]. In contrast to widely studied biodegradable polymers such as polylactic acid (PLA), the flame retardancy of PCL has received minimal attention in the literature and has predominantly been addressed only within PLA/PCL blend systems. It should be noted that flame-retardant PLA/PCL systems reported are typically PLA-rich blends, with PLA contents commonly ranging between 50 and 80 mass%, while PCL is primarily introduced to improve toughness. Flame retardancy in 50/50 PLA/PCL was enhanced using 10 mass% ammonium polyphosphate (APP) and 8 mass% carbon nanotubes (CNTs) modified with 1.6 mass% imidazolium-functionalised polyurethane (IPU), achieving a UL-94 V-0 classification and a 39% reduction in peak heat release rate in cone calorimetry compared to the APP-only composite [19]. A hybrid system combining MXene and nitrogen-phosphorus-modified bamboo charcoal (BC-NPA) in 80/20 PLA/PCL blends improved both mechanical performance and fire resistance, increasing the LOI to 32.9% and reaching a UL-94 V-0 classification at 2.5 mass% MXene content [20]. PLA/PCL blends filled with $CaCO_3$ for 3D printing showed enhanced crystallinity and thermal stability, achieving UL-94 V-0 classification together with improved impact toughness and structural integrity [21]. To the best of the authors' knowledge, however, the flame retardant modification of PCL in filament form, particularly, with relevance to additive manufacturing and structural interlayer applications, has not yet been reported, which is also reflected by the absence of PCL-based systems in recent comprehensive reviews on the fire behavior of 3D-printed polymer composites [22]. This research gap is further underscored by a comprehensive review on PCL published in 2025, which provides an in-depth overview of PCL synthesis, properties and applications, yet does not consider flame retardancy-related aspects [23].

The aim of the present research is the development and characterization of PCL-based, flame-retardant-modified filaments that are compatible with additive manufacturing technologies and can be successfully integrated as interlayer materials into polymer composite structures, where the interlayer is intended to promote pseudo-ductile behavior and enhanced toughness while simultaneously providing improved flame retardancy. Within this work, neat and flame-retardant-containing PCL filaments were produced, enabling a comprehensive evaluation of their thermal behavior, stability, and mechanical performance, with a particular emphasis on the influence of the flame retardants on the intrinsic properties of PCL, as well as on its processability. The manufactured filaments were incorporated as interlayer elements into CFRP composite laminates. The investigation of the composites focused on their behavior under fire exposure, examining how the PCL-based interlayer affects damage evolution processes under thermal loading and the preservation of structural integrity. Based on the results, the role of

15480585, 2026, 4, Downloaded from https://4spepublications.onlinelibrary.wiley.com/doi/10.1002/vnl.70126 by Budapest University of Technology and Economics, Wiley Online Library on [02/08/2026]. See the Terms and Conditions (https://onlinelibrary.wiley.com/terms-and-conditions) on Wiley Online Library for rules of use; OA articles are governed by the applicable Creative Commons License

the interlayer in composite fire performance was systematically evaluated. The findings support multifunctional composite systems in which the interlayer provides both structural and safety functions, highlighting the additively manufactured interlayers as a promising pathway for developing advanced polymer composite structures meeting stringent safety requirements.

2 | Materials and Methods

2.1 | Materials

PCL ESUN-PCL600C (Shenzhen Esun Industrial Co. Ltd., Shenzhen, China) was used as a thermoplastic interlaminar modifier. The semi-crystalline aliphatic polyester has a melting temperature of 58°C–62°C, a molecular weight of 63,000–72,000 g/mol, and a decomposition temperature of approximately 260°C. APP was applied as a halogen-free flame retardant using NORD-MIN JLS APP (Nordmann, Rassmann GmbH, Hamburg, Germany). The material contains 31.0–32.0 mass% phosphorus and 14.0–15.0 mass% nitrogen, with an average particle size of ~15 μm and low water solubility. Expandable graphite (EG) GHL PX 92-1 HT 270 (Georg H. Luh GmbH, Walluf, Germany) was used as a synergistic flame-retardant additive. The graphite grade has a minimum carbon content of 92 mass%, a starting expansion temperature of ≥ 270°C, and an expansion volume of at least 40 mL/g. The matrix material was IPOX MR 3010 (IPOX Chemicals Kft., Budapest, Hungary), a DGEBA-based epoxy resin, cured with IPOX MH 3124 amine-based curing agent at a weight ratio of 100:35. Unidirectional carbon fiber fabric PX35FBUD0300 (Zoltek Zrt., Nyergesújfalu, Hungary) with an areal weight of 309 g/m^2, consisting of Panex35 50 k rovings, was used as reinforcement.

2.2 | Filament Production

PCL filaments were produced using an LTE 26–44 corotating twin-screw extruder (Labtech Engineering Ltd., Samutprakarn, Thailand) with a screw diameter of 26 mm and an L/D ratio of 44. The barrel temperatures were set to 60°C–70°C from hopper to die, with a die temperature of 70°C. The screw speed was 25 rpm and the volumetric feeder speed was 5 rpm. A single-filament die with a 2.5 mm spinneret diameter was used.

The extruder was connected to a custom-made filament production line comprising two water-cooling tanks (total length: 3.3 m), a laser diameter measurement unit (ODAC 13TRIO, Zumbach Electronic AG, Orpund, Switzerland), a drawing unit and a take-up unit. The first cooling tank was positioned 105 mm from the die, allowing the filament diameter to be reduced to the target value of 1.75 mm before entering the cooling water. Cooling water temperatures were maintained at 13.5°C for unfilled PCL and 20.5°C for the PCL_5%EG and PCL_10%APP filaments. The filament remained fully submerged during cooling.

After cooling, residual water was removed with compressed air and the filament diameter was measured by a three-axis laser system. Under the applied processing conditions, filaments with a diameter of 1.75 ± 0.2 mm were produced. The filament was drawn through the line by rubber-coated rollers at 4.44 m/min and wound onto a spool at a matching take-up speed.

2.3 | Methods of Preparation

Custom-made polymer filaments were used in this study. Test specimens for thermal, flammability, and mechanical characterization were manufactured from the produced filaments by fused filament fabrication (FFF) technology. PCL-based interlayer materials were fabricated by FFF and applied in neat and flame-retardant-modified forms. For flame-retarded systems, formulations containing 5 mass% EG or 10 mass% APP were prepared. The calculated mass percentage values are presented in Table 1.

The additive content in the filaments was chosen based on preliminary fabrication trials, as higher loadings led to poor dispersion of graphite or APP, resulting in agglomerates that compromised filament drawability and extrusion quality. The interlayers were printed with a grid-pattern structure using infill ratios of 50% and 75% (Figure 1). The patterned interlayers were

TABLE 1 | Calculated mass percentages of the interlayer, flame-retardant additive, and phosphorus content relative to the total composite sample mass.

Sample	Sample mass (g)	Interlayer mass (g)	Interlayer flame retardant content (mass%)	Interlayer content (mass%)	Flame retardant content in the total sample (mass%)	P content in the total sample (mass%)
Reference	33.92	0	0	0	0	0
PCL50	37.20	1.11	0	2.98	0	0
PCL75	36.18	1.85	0	5.11	0	0
APP50	48.63	1.11	10	2.28	0.23	0.072
APP75	41.83	1.85	10	4.42	0.44	0.139
EG50	35.82	1.11	5	3.10	0.15	0
EG75	40.13	1.85	5	4.61	0.23	0

15480585, 2026, 4, Downloaded from https://4spepublications.onlinelibrary.wiley.com/doi/10.1002/vnl.70126 by Budapest University of Technology and Economics, Wiley Online Library on [02/08/2026]. See the Terms and Conditions (https://onlinelibrary.wiley.com/terms-and-conditions) on Wiley Online Library for rules of use; OA articles are governed by the applicable Creative Commons License

directly printed onto carbon fiber fabrics before composite manufacturing. The interlayer was printed only on the top surface of the carbon fiber reinforcement. The thickness of the printed PCL interlayer was 0.4 mm. Composite laminates were produced by vacuum infusion (Figure 2). The laminates consisted of six plies of carbon fiber reinforcement (Figure 1). Flat glass molds covered with polyethylene terephthalate (PET) films were used, with peel plies placed on both sides of the laminate to facilitate demoulding. A resin distribution medium was applied above the peel plies to ensure uniform resin flow. The printed interlayer patterns were positioned within the laminate, integrated into the uppermost ply during layup. A vacuum bag was assembled to provide uniform consolidation and high fiber volume fraction. The fiber volume fraction of the composites was approximately 60 vol%. A vacuum pressure of 0.6 bar was applied, and the laminates were cured for 3 h in a drying oven at 90°C. Under these processing conditions, the PCL interlayers were only partially dissolved in the epoxy matrix. After curing, test specimens were cut from the laminates using a diamond disc saw (Diadisc 5200, Mutronic Präzisionsgerätebau GmbH, Rieden, Germany) in accordance with the relevant testing standards.

For TGA, DSC, and PCFC analyses, the samples were prepared by cutting small segments from the produced filaments, which

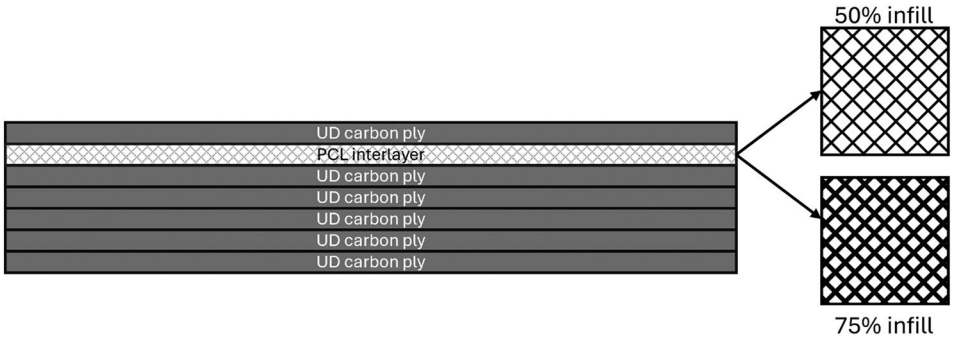

FIGURE 1 | Schematic representation of the laminate structure and interlayer infill design.

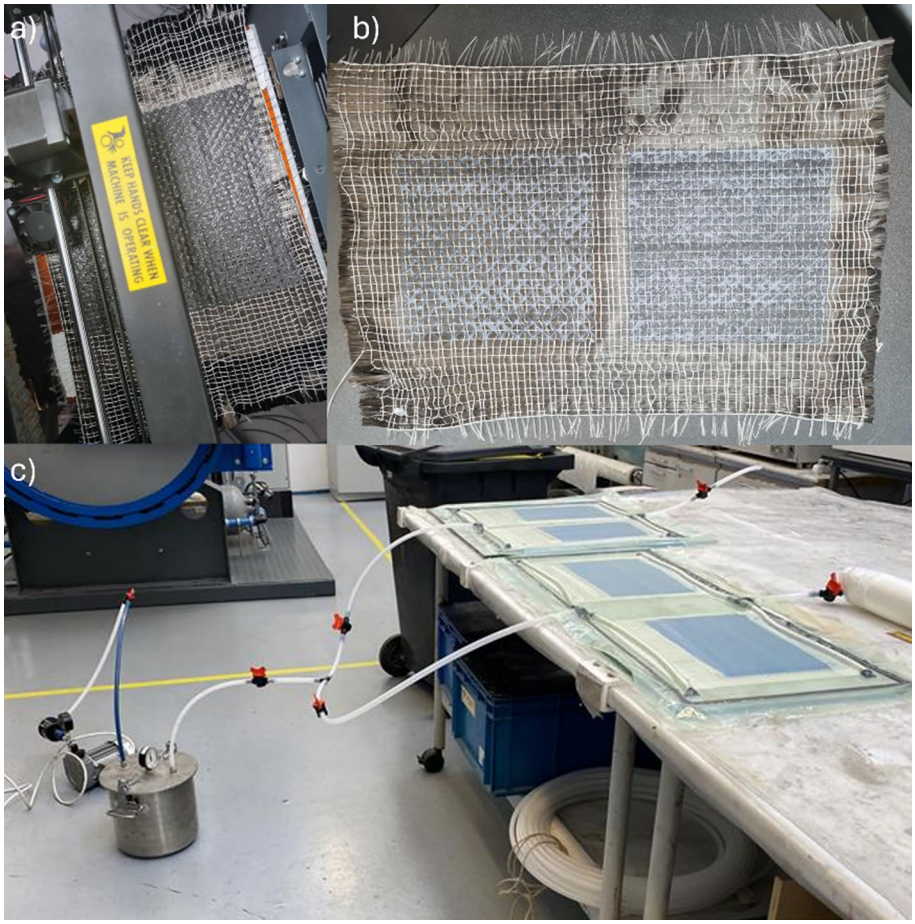

FIGURE 2 | Illustration of the fabrication process: (a) printing of the PCL interlayer onto the UD carbon fiber reinforcement; (b) printed interlayer patterns with 50% and 75% infill; (c) vacuum infusion process.

15480585, 2026, 4, Downloaded from https://4spepublications.onlinelibrary.wiley.com/doi/10.1002/vnl.70126 by Budapest University of Technology and Economics, Wiley Online Library on [02/08/2026]. See the Terms and Conditions (https://onlinelibrary.wiley.com/terms-and-conditions) on Wiley Online Library for rules of use; OA articles are governed by the applicable Creative Commons License

were used directly for the measurements without further processing. For cone calorimetry measurements, PCL-based samples were prepared by FFF using the produced filaments.

For tensile and flexural testing, standardized specimens were manufactured by FFF using the produced filaments.

2.4 | Testing and Characterization

2.4.1 | TGA

We analyzed the thermal stability of the samples using a Q500 thermogravimetric analyzer (TA Instruments, New Castle, DE, USA) between 30°C and 800°C at a heating rate of 20°C/min in a nitrogen atmosphere with a 30 mL/min flow rate. The samples weighed 5–10 mg, and the data were evaluated with the TA Universal Analysis program.

2.4.2 | DSC

We determined the thermal transitions and the degree of crystallinity of the investigated materials by differential scanning calorimetry (DSC) using a Q2000 DSC instrument (TA Instruments, New Castle, DE, USA) in the temperature range from −90°C to 180°C at a constant heating and cooling rate of 10°C/min. A heating–cooling–heating thermal programme was applied to eliminate thermal history effects prior to evaluation. Approximately 5–10 mg of each sample was placed in aluminum pans and analyzed under a nitrogen atmosphere with a purge gas flow rate of 50 mL/min.

The degree of crystallinity (X_c) was calculated using the following equation:

$$X_c(\%) = \frac{\Delta H_m}{w_{\mathrm{PCL}} \cdot \Delta H_m^0} \cdot 100 \quad (1)$$

where $\Delta H_m$is the melting enthalpy obtained from DSC, $w_{\mathrm{PCL}}$is the mass fraction of PCL in the sample, and $\Delta H_m^0 = 139.5\,\mathrm{J/g}$ [24] is the theoretical melting enthalpy of 100% crystalline PCL.

2.4.3 | Pyrolysis–Combustion Flow Calorimetry (PCFC)

We evaluated the flammability of the materials using pyrolysis–combustion flow calorimetry (PCFC) with a Fire Testing Technology instrument (East Grinstead, UK) according to ASTM D7309 standard, at a heating rate of 1°C/s on 2–5 mg samples, with a maximum pyrolysis temperature of 750°C and a combustion chamber temperature of 900°C. Nitrogen and oxygen were supplied at flow rates of 80 mL/min and 20 mL/min, respectively.

2.4.4 | Cone Calorimetry

We investigated the combustion behavior of neat PCL, flame-retarded PCL, and composite specimens incorporating PCL-based interlayers using a TCC 918 cone calorimeter (NETZSCH TAURUS Instruments GmbH, Weimar, Germany) in accordance with ISO 5660-1. Square specimens with a surface area of 100 mm × 100 mm were exposed to an external heat flux of 50 kW/m^2 and ignited using a spark igniter. The following parameters were determined from the cone calorimetric measurement: time to ignition (TTI), peak heat release rate (pHRR), time to pHRR (t_{pHRR}), total heat release (THR), total smoke production (TPS), maximal average rate of heat emission (MARHE), effective heat of combustion (EHC), residual mass, and the total emission of CO and CO_2.

2.4.5 | Tensile Test

Tensile tests were carried out using a Zwick Z250 universal testing machine (ZwickRoell GmbH, Ulm, Germany) equipped with a 20 kN load cell. Standardized dog-bone–shaped tensile specimens were tested in accordance with EN ISO 527-2, Type 5A (Figure 3). The specimens were clamped using 20 kN capacity screw-action (vice-type) grips, and the gauge length was set to 50 mm. Tensile loading was applied at a constant crosshead speed of 20 mm/min, while the modulus was determined at a rate of 1 mm/min. Prior to testing, all relevant geometric parameters of the specimens were measured. The tensile tests were performed up to 50% strain.

2.4.6 | Flexural Tests

Flexural tests were conducted using a Zwick Z250 universal testing machine (ZwickRoell GmbH, Ulm, Germany) equipped with a three-point bending fixture and a 20 kN load cell. The tests were performed in accordance with EN ISO 178. Standard rectangular specimens with nominal dimensions of 80 mm × 10 mm × 4 mm were used. The support span was set to 64 mm. Flexural loading was applied at a constant crosshead speed of 10 mm/min, while the modulus was determined at a rate of 1 mm/min. Prior to testing, all relevant geometric parameters of the specimens were measured.

2.4.7 | Tensile Impact Tests

Tensile impact tests were performed with a Resil Impactor Junior pendulum (Ceast, Torino, Italy). The tests were carried out according to ISO 8256, Method A. Type 2 standardized dog-bone–shaped tensile specimens were tested in order to evaluate

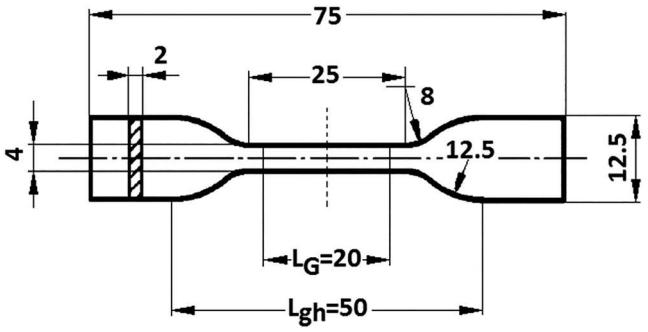

FIGURE 3 | Dimensions (mm) of the ISO 527/2-5A specimen.

15480585, 2026, 4, Downloaded from https://4spepublications.onlinelibrary.wiley.com/doi/10.1002/vnl.70126 by Budapest University of Technology and Economics, Wiley Online Library on [02/08/2026]. See the Terms and Conditions (https://onlinelibrary.wiley.com/terms-and-conditions) on Wiley Online Library for rules of use; OA articles are governed by the applicable Creative Commons License

the impact resistance of the materials. The measurements were conducted with a 15 J hammer using a crosshead with a mass of 30 g. A toss energy of 0.46 J was used as a correction factor according to the standard.

3 | Results and Discussion

3.1 | Thermal and Flammability Properties

3.1.1 | Thermogravimetric Analysis

The thermal stability of the additives, PCL and PCL_5%EG, PCL_10%APP samples was examined with TGA. The results are summarized in Figure 4 and Table 2.

The temperature corresponding to 5% mass loss ($T_{-5\%}$) of neat PCL was 377°C, indicating good initial thermal stability of the polymer. The incorporation of EG reduced $T_{-5\%}$ to 317°C, while the PCL sample containing APP exhibited a $T_{-5\%}$ value of 360°C. The reduced onset decomposition temperature of PCL_10%APP is consistent with the early degradation of APP, which is generally associated with the formation of phosphorus-containing species that promote char formation in the polymer matrix.

The temperature at 50% mass loss ($T_{-50\%}$) for neat PCL was 415°C. The presence of EG reduced $T_{-50\%}$ to 396°C, while a further decrease to 386°C was observed for the APP-containing sample. Although APP accelerates the mass loss process, APP exhibited a residual mass of 42.4% at 800°C. Based on the 10 mass% APP content of the PCL_10%APP sample, approximately 4.2% residue would be expected from the additive alone. The experimentally observed residue of 6.6% therefore suggests that APP promotes additional char formation from the PCL matrix. Although EG exhibited a residual mass of 90.7% at 800°C when tested alone, no measurable residue was detected for PCL_5%EG under the applied TGA conditions. This result was reproducibly observed in repeated measurements, and no visible residue remained in the platinum pan after the tests. A possible explanation is that the highly expanded and mechanically fragile graphite structure formed during decomposition was partially removed from the open sample pan by the nitrogen purge gas. Therefore, the residual mass determined by TGA may underestimate the actual amount of expanded graphite formed during thermal degradation. Consequently, the flame-retardant action of EG is more appropriately attributed to its expansion behavior and the formation of a protective barrier during thermal exposure than to the residual mass measured at 800°C.

The maximum mass loss rate (dTG_{max}) of neat PCL was 2.13%/°C. The addition of EG decreased this value to 1.56%/°C, whereas APP increased it to 2.58%/°C, indicating different degradation mechanisms. The temperature corresponding to the maximum mass loss rate (T_{dTGmax}) was 418°C for neat PCL

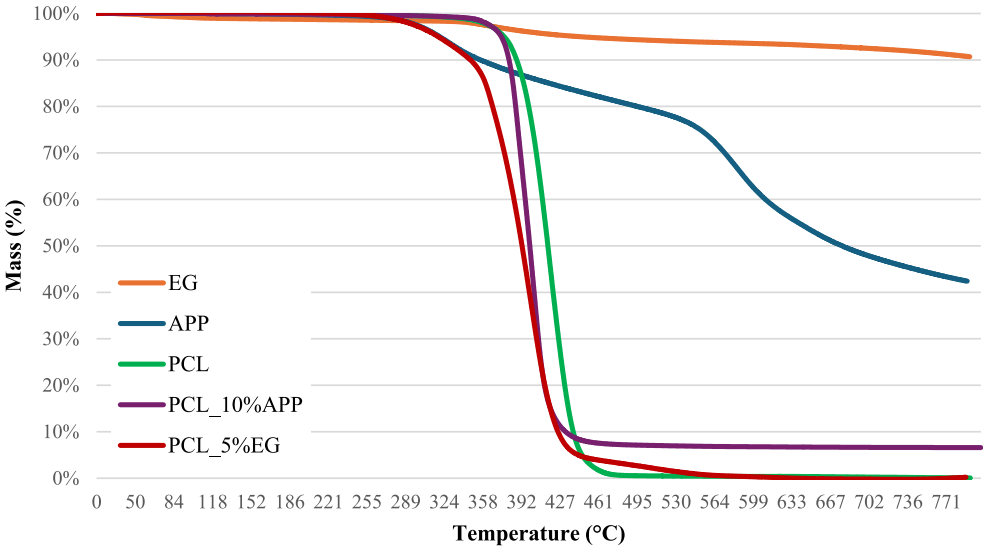

FIGURE 4 | Thermogravimetric analysis (TGA) curves of the flame retardants, PCL, and PCL containing flame retardant additives.

TABLE 2 | Summary of TGA results of the flame retardants, PCL, and PCL containing flame retardant additives.

Sample	$T_{-5\%}$ (°C)	$T_{-50\%}$ (°C)	dTG_{max} (%/°C)	T_{dTGmax} (°C)	Residual mass at 800°C (%)
EG	445	—	0.04	362	90.7
APP	321	677	0.30	588	42.4
PCL	377	415	2.13	418	0
PCL_5%EG	317	396	1.56	404	0
PCL_10%APP	360	386	2.58	390	6.6

Abbreviations: dTG_{max} (%/°C): maximum mass loss rate; $T_{-5\%}$ (°C): temperature at 5% mass loss; $T_{-50\%}$ (°C): temperature at 50% mass loss; T_{dTGmax} (°C): temperature at the maximum mass loss rate.

15480585, 2026, 4, Downloaded from https://4spepublications.onlinelibrary.wiley.com/doi/10.1002/vnl.70126 by Budapest University of Technology and Economics, Wiley Online Library on [02/08/2026]. See the Terms and Conditions (https://onlinelibrary.wiley.com/terms-and-conditions) on Wiley Online Library for rules of use; OA articles are governed by the applicable Creative Commons License

and decreased to 404°C and 390°C upon the incorporation of EG and APP, respectively.

Overall, the observed decrease in decomposition temperatures reflects additive-specific degradation pathways rather than reduced flame-retardant efficiency. In particular, enhanced char formation (as observed for APP-containing systems) is indicative of effective flame-retardant action, whereas EG acts predominantly through physical expansion and barrier formation, which is not directly reflected in the residual mass measured by TGA.

3.1.2 | Differential Scanning Calorimetry

Based on the DSC results (Table 3), it can be concluded that the applied flame-retardant additives have a pronounced effect on the crystallization behavior of PCL, while the melting temperature remains essentially unchanged.

For the neat PCL sample, the maximum of the crystallization peak appears at 22.96°C. This relatively low crystallization temperature is consistent with the literature data for PCL and represents a technological limitation during processing. The melting enthalpy of the neat PCL sample was determined as 65.08 J/g, resulting in a degree of crystallinity of 46.7%.

For the sample containing 10 mass% APP, the crystallization peak maximum is detected at 34.12°C. This result suggests a strong nucleating effect of APP, further enhancing the crystallization kinetics and facilitating the formation of the crystalline structure at higher temperatures. The melting enthalpy of this sample was 62.83 J/g, which corresponds to a crystallinity of 50.1%.

In the case of the sample containing 5 mass% EG, a significant shift in the crystallization temperature is observed. The crystallization peak maximum increases to 40.80°C, corresponding to an elevation of approximately 17°C compared to the unfilled PCL, which is the highest value among the investigated samples. This shift indicates that EG acts as an efficient heterogeneous nucleating agent, promoting the earlier onset of crystallization. The melting enthalpy reached 73.70 J/g for this sample, resulting in the highest crystallinity of 55.6% among the investigated materials.

The melting behavior of all samples occurs within a similar temperature range, with melting peaks appearing between 56°C and 61°C. No significant influence of the additives on the melting temperature can be identified. This indicates that the additives predominantly affect the crystallization process, while the thermodynamic stability of the formed crystalline phase remains largely unchanged.

Overall, both EG and APP beneficially increase the crystallization temperature of PCL, which is advantageous from a processing perspective, particularly in manufacturing environments where cooling capacity is limited. In addition to the shift in crystallization temperature, both additives also increased the degree of crystallinity, further confirming their nucleating effect. The most pronounced increase was observed for the EG-containing sample.

TABLE 3 | DSC results and calculated crystallinity of reference and flame-retarded PCL samples.

Sample	T_c (°C)	T_m (°C)	ΔH_m (J/g)	w_{PCL}	X_c (%)
PCL	22.96	56.38	65.08	1.00	46.7
PCL_10%APP	34.12	57.68	62.83	0.90	50.1
PCL_5%EG	40.80	56.96	73.70	0.95	55.6

Abbreviations: *Tc* (°C): temperature of crystallization peak, T_m (°C): melting point, w_{PCL}: mass fraction of PCL, X_C (%): degree of crystallinity, ΔH_m (J/g): melting enthalpy.

3.1.3 | Pyrolysis Combustion Flow Calorimetry

The flammability behavior of neat poly(ε-caprolactone) (PCL) and PCL systems containing 10 mass% APP or 5 mass% EG (EG) was investigated using pyrolysis combustion flow calorimetry (PCFC). The main PCFC parameters are summarized in Table 4. In the present evaluation, particular attention is given to the temperature at maximum heat release (T_p), which characterizes the temperature range of the dominant decomposition process.

For neat PCL, the T_p value is 437°C, representing the highest value among the investigated systems. This indicates that the intensive thermal decomposition of PCL occurs at a relatively high temperature under PCFC conditions. The addition of flame retardants results in a clear decrease in T_p in all cases. In the presence of APP, T_p shifts to a significantly lower temperature by approximately 46°C, whereas the incorporation of EG leads to a smaller shift of about 34°C toward lower temperatures.

The shift of T_p to lower temperatures suggests that the onset of intensive decomposition occurs earlier in the presence of the additives. For APP, the more pronounced effect can be attributed to the formation of acidic phosphorus-containing species during thermal degradation, which may promote chain scission of the polyester backbone and accelerate the release of volatile decomposition products. In contrast, the more moderate effect observed for EG is consistent with the fact that EG primarily

TABLE 4 | Pyrolysis combustion flow calorimetry (PCFC) results of PCL and PCL containing flame retardant additives.

Sample	Mass (mg)	pHRR (W/g)	THR (kJ/g)	HRC (J/g °C)	T_p (°C)	Residue (%)
PCL	3.63	635	27	652	437	0
PCL_10%APP	4.70	1077	21	1082	392	3.1
PCL_5%EG	2.90	1003	25	1022	404	6.8

Note: Average standard deviation of the measure PCFC values: pHRR: ±20; THR: ±3; HRC: ±10; T_p: ±5; residue: ±2.
Abbreviations: HRC, heat release capacity; pHRR, peak heat release rate; THR, total heat release; T_p, temperature at peak heat release rate.

15480585, 2026, 4, Downloaded from https://4spepublications.onlinelibrary.wiley.com/doi/10.1002/vnl.70126 by Budapest University of Technology and Economics, Wiley Online Library on [02/08/2026]. See the Terms and Conditions (https://onlinelibrary.wiley.com/terms-and-conditions) on Wiley Online Library for rules of use; OA articles are governed by the applicable Creative Commons License

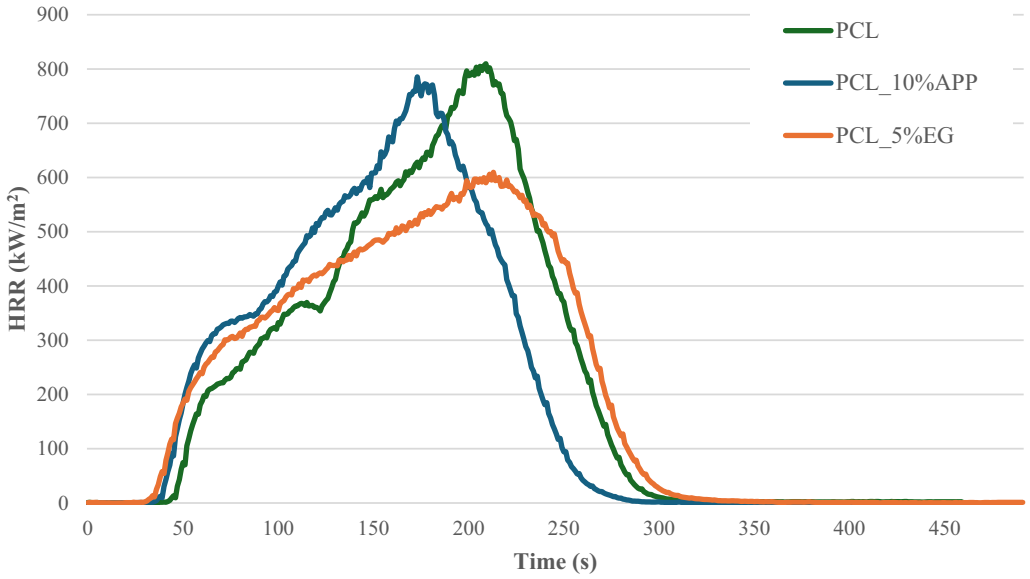

FIGURE 5 | Heat release rate (HRR) as a function of time for PCL and PCL containing flame retardant additives obtained from cone calorimeter tests.

acts through physical barrier formation, a mechanism that cannot fully develop under the micro-scale conditions of the PCFC measurement.

Both APP and EG increase the peak heat release rate (pHRR) compared to neat PCL, reflecting a more intense heat release at the early stages of decomposition. At the same time, the total heat release (THR) is reduced for APP and, to a lesser extent, for EG, indicating that the overall energy available for combustion is limited despite the higher instantaneous heat release. The increase in heat release capacity (HRC) observed for both APP- and EG-containing PCL systems further indicates that flame retardants promote a more intense but temporally concentrated heat release during the main decomposition event. In the case of APP, this effect is consistent with acid-catalyzed chain scission, while for EG it reflects the limited effectiveness of barrier formation under PCFC conditions. These results indicate that, under the applied experimental conditions, the investigated flame retardants do not enhance the thermal stability of the PCL matrix but rather shift the main decomposition process to a lower temperature range.

3.1.4 | Cone Calorimetry

3.1.4.1 | Results of the Flame Retarded PCL Matrix Specimens. To assess the flammability performance of the reference and flame retarded PCL matrix specimens manufactured by FFF, we conducted cone calorimeter tests. These experiments provided a comparative evaluation of the fire behavior of the PCL filament base materials, with particular emphasis on heat release characteristics and mass loss behavior during combustion. The measured parameters allow an objective comparison of the effectiveness of the applied additives and support the interpretation of their dominant flame-retardant mechanisms.

For the evaluation, heat release rate as a function of time (HRR–time) and mass loss as a function of time (mass loss–time) diagrams were generated (Figures 5 and 7). The quantitative comparison was primarily based on the peak heat release rate (pHRR), as this parameter directly characterizes the combustion intensity and the fire hazard of the material. A summary of the numerical results is provided in the corresponding table (Table 5).

The HRR–time curves of the investigated samples reveal distinct differences in combustion behavior. The neat PCL specimen exhibits a rapid increase in heat release rate, resulting in a pronounced peak with a pHRR of 810 kW/m^2. This behavior indicates rapid thermal decomposition of the molten polymer and intensive release of combustible volatiles.

For the PCL_10%APP formulation the pHRR is slightly reduced to 758 kW/m^2. Although APP modifies the combustion process, the total heat release remains high, suggesting that under the applied conditions, the APP-driven condensed-phase does not form a sufficiently continuous and mechanically stable protective structure to suppress the heat release peak effectively.

The PCL_5%EG formulation exhibits the most favorable fire performance among the tested samples. The pHRR is significantly reduced to 610 kW/m^2, and the HRR curve shows a broader and less pronounced peak. This behavior can be attributed to the expansion of graphite during heating, which forms a physical barrier that limits heat transfer and volatile release. The flatter HRR profile indicates a less intense combustion process.

The mass–time curves of the three samples show a generally similar overall trend. Following ignition, a steep mass loss phase is observed for all specimens, followed by a gradual transition toward a plateau as combustion progresses. The

15480585, 2026, 4, Downloaded from https://4spepublications.onlinelibrary.wiley.com/doi/10.1002/vnl.70126 by Budapest University of Technology and Economics, Wiley Online Library on [02/08/2026]. See the Terms and Conditions (https://onlinelibrary.wiley.com/terms-and-conditions) on Wiley Online Library for rules of use; OA articles are governed by the applicable Creative Commons License

TABLE 5 | Summary of cone calorimeter results for PCL and PCL containing flame retardant additives.

Sample	TTI (s)	MARHE (kW/m²)	pHRR (kW/m²)	t_{pHRR} (s)	THR (mJ/m²)	TSP (m²/m²)	EHC (mJ/m²)	Residual mass (%)
PCL	49	387	810	209	104	1180	25.1	1
PCL_10%APP	41	399	758	173	96	1995	26.8	9
PCL_5%EG	38	368	609	213	102	1223	28.1	4

Note: Average standard deviation of the measured cone calorimetry values: TTI: ±3; pHRR: ±30; t_{pHRR}: ±5; THR: ±3; residual mass: ±2; TSP: ±20.
Abbreviations: EHC, effective heat of combustion; MARHE, maximum average rate of heat emission; pHRR, peak heat release rate; THR, total heat release; t_{pHRR}, time to peak heat release rate; TSP, total smoke production; TTI, time to ignition.

FIGURE 6 | The residues remaining after cone calorimeter testing: (a) PCL, (b) PCL_10%APP, (c) PCL_5%EG.

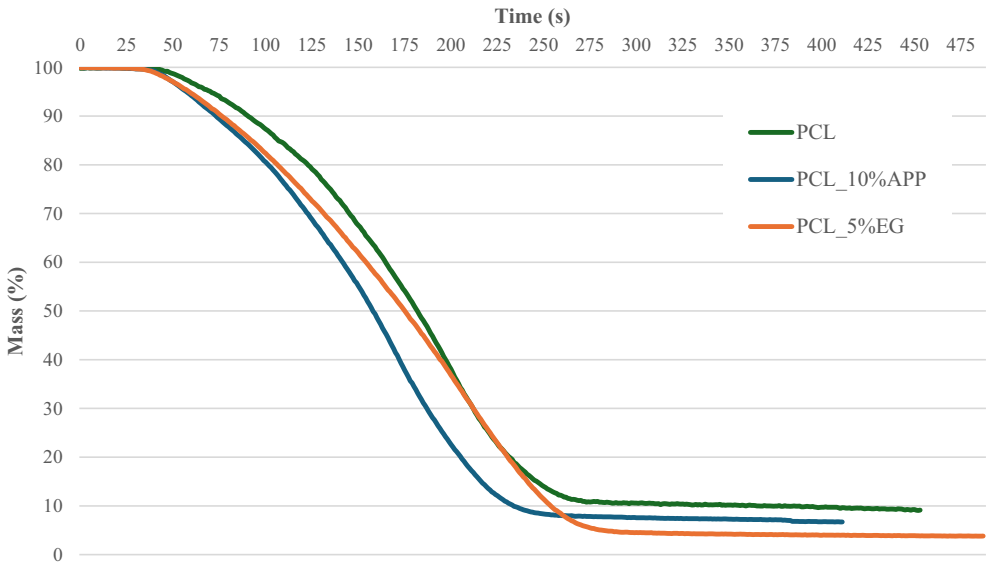

FIGURE 7 | Mass as a function of time for PCL and PCL containing flame retardant additives determined by cone calorimeter tests.

similarities in curve shape indicate that no pronounced differences in the mass loss dynamics can be clearly distinguished between the systems.

The residual mass values indicate that the PCL matrix is almost completely consumed during combustion, with the remaining residue corresponding approximately to the initial additive content in both formulations. This suggests that PCL melts and decomposes before the flame-retardant additives can exert a significant protective effect under the applied test conditions. Overall, the mass loss results suggest that the applied additives do not strongly alter the mass loss rate profile under these test conditions. Instead, their influence is more clearly reflected in the residual phase characteristics (Figure 6) and—consistent with the HRR results—in the modification of heat release intensity (Figure 5).

15480585, 2026, 4, Downloaded from https://4spepublications.onlinelibrary.wiley.com/doi/10.1002/vnl.70126 by Budapest University of Technology and Economics, Wiley Online Library on [02/08/2026]. See the Terms and Conditions (https://onlinelibrary.wiley.com/terms-and-conditions) on Wiley Online Library for rules of use; OA articles are governed by the applicable Creative Commons License

The main fire reaction parameters derived from the cone calorimeter measurements—including TTI, pHRR, THR, MARHE, and residual mass—are summarized in the corresponding table (Table 5). These data provide a compact overview of the influence of flame retardants on the combustion behavior of the printed samples.

Based on the comparison of pHRR values, the PCL_5%EG formulation demonstrates the most effective reduction in combustion intensity, while neat PCL exhibits the most severe fire behavior. The PCL_10%APP formulation shows an intermediate response, characterized by a modest reduction in pHRR and an increased residual mass. Overall, the results indicate that EG primarily reduces peak heat release via barrier formation, whereas APP predominantly promotes condensed-phase residue formation.

3.1.4.2 | Results of the Flame Retarded PCL Composite Specimens. The purpose of the cone calorimetry study was to comparatively evaluate the fire behavior of carbon fiber–reinforced composite specimens incorporating different flame-retardant interlayers, with particular emphasis on heat release characteristics and the effectiveness of the formed protective layers. The evaluation was based on the heat release rate (HRR)–time and mass loss–time curves, complemented by the characteristic fire parameters summarized in Table 6.

The HRR–time curves (Figure 8) reveal a complex, multi-stage combustion process for all investigated samples. Following ignition, a rapid increase in heat release rate is observed, corresponding to intensive flaming combustion. This phase is followed by a lower-intensity stage associated with char formation and smoldering. In several cases, a secondary increase in HRR appears at later times, which can be attributed to cracking of the protective layer and partial re-ignition of the underlying material.

The reference composite exhibits a relatively high peak heat release rate (pHRR ≈346 kW/m^2) combined with a short combustion duration. This behavior indicates rapid heat release after ignition and limited formation of an effective thermal barrier.

TABLE 6 | Summary of cone calorimeter results.

Sample	TTI (s)	MARHE (kW/m^2)	pHRR (kW/m^2)	t_{pHRR} (s)	THR (MJ/kg)	TSP (m^2/kg)	EHC (MJ/kg)	Residual mass (%)
Ref.	43	188	346	68	11.7	532	27.6	58
PCL_50	32	205	303	95	12.7	595	27.1	53
PCL_75	36	215	343	102	12.4	587	27.1	54
APP_50	33	255	379	119	15.3	791	26.3	42
APP_75	23	250	370	131	13.4	497	26.2	49
EG_50	31	211	311	56	12.6	336	27.7	55
EG_75	33	222	329	131	13.2	429	26.5	50

Note: Average standard deviation of the measured cone calorimetry values: TTI: ±3; pHRR: ±30; t_{pHRR}: ±5; THR: ±3; residual mass: ±2.
Abbreviations: EHC, effective heat of combustion; MARHE, maximum average rate of heat emission; pHRR, peak heat release rate; THR, total heat release; t_{pHRR}, time to peak heat release rate; TSP, total smoke production; TTI, time to ignition.

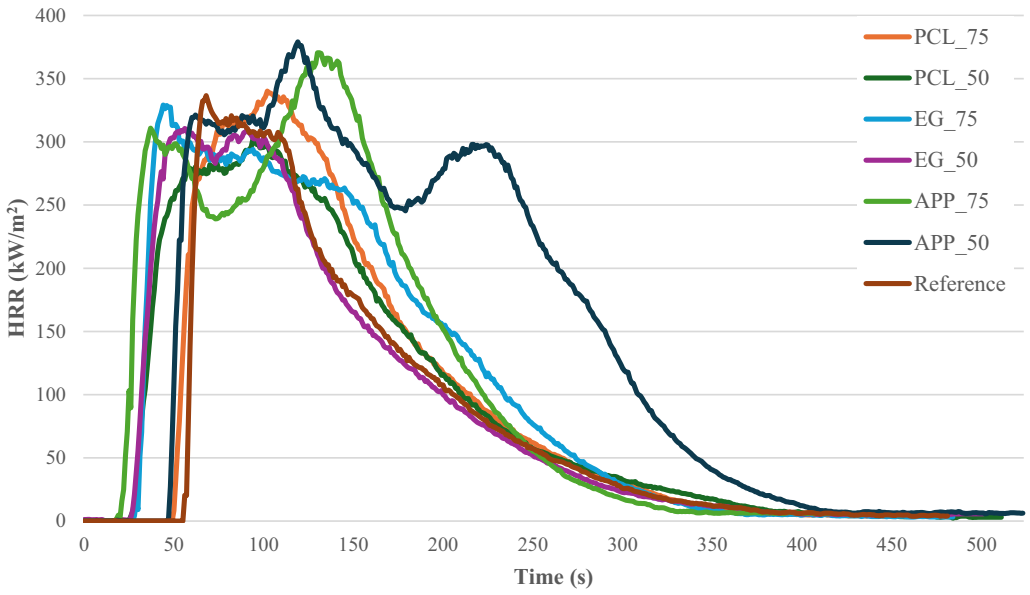

FIGURE 8 | Heat release rate of composite specimens containing flame-retardant interlayers.

15480585, 2026, 4, Downloaded from https://4spepublications.onlinelibrary.wiley.com/doi/10.1002/vnl.70126 by Budapest University of Technology and Economics, Wiley Online Library on [02/08/2026]. See the Terms and Conditions (https://onlinelibrary.wiley.com/terms-and-conditions) on Wiley Online Library for rules of use; OA articles are governed by the applicable Creative Commons License

The samples containing a PCL interlayer show a moderate reduction in pHRR, while the overall combustion process becomes more prolonged. This suggests that melting and thermal degradation of the PCL layer provide a temporary heat-shielding effect; however, no mechanically stable and continuous char layer is formed. Increasing the infill density does not lead to a clear improvement in fire performance, as the slight increase in time to ignition is accompanied by an increase in pHRR.

The APP–containing samples exhibit the least favorable fire behavior. In both infill configurations, the pHRR values exceed that of the reference sample, and the secondary heat release stage is particularly pronounced. These results indicate that although APP promotes charring, as also supported by the increased char residue observed in the TGA measurements, the resulting protective layer is insufficient to effectively suppress heat release. This limited effectiveness can be attributed to the relatively low APP content introduced through the localized PCL interlayer and to the melting of the PCL phase during combustion, which may hinder the formation of a continuous and mechanically stable intumescent barrier. During cone calorimetry, the PCL interlayer melts before substantial char development occurs and may partially flow out from the specimen edges, hindering the formation of a continuous, compact and mechanically stable intumescent barrier. Consequently, although charring occurs, the resulting protective layer does not provide effective insulation against heat and mass transfer. Higher infill density leads to a slower but more sustained combustion process, further suggesting insufficient integrity of the protective layer.

In contrast, the samples incorporating EG display a more favorable combustion behavior. A more pronounced reduction in pHRR is observed, particularly at lower infill density, which can be attributed to the formation of an expanded graphite layer acting as an efficient physical thermal barrier. At higher infill density, a similar HRR trend is observed; however, the appearance of a minor secondary peak indicates partial destabilization of the protective layer during the later stages of combustion.

PCL, APP, and EG denote the type of additive, while the numbers (50 and 75) indicate the infill density (%) of the printed interlayer structure.

As can be observed from the mass–time curves (Figure 9), the composites containing neat PCL interlayers exhibited lower residual mass compared to the reference sample. This result was expected, since PCL is a polymer with lower thermal stability that does not form a significant solid residue during thermal decomposition.

In the case of the flame-retarded systems, it was expected that the EG or APP additives would partially compensate for the lower residual mass associated with the presence of PCL. However, this effect was only minimally observed for the EG_50 sample, while in the other cases the residual mass decreased further. It is likely that the concentration of the flame-retardant additives within the overall composite system was too low for their residue-forming effect to be fully manifested (Table 1).

The characteristic fire parameters summarized in Table 6 quantitatively confirm the trends observed in the HRR and mass loss curves. Due to the unavoidable differences in sample mass and thickness due to the introduction of the interlayer, parameters directly related to the exposed surface area (pHRR, MARHE, TTI) were evaluated in their original form, whereas THR and TSP were additionally considered on a mass-specific basis to allow a more meaningful comparison of material-related fire load and smoke production.

The EG–containing samples exhibit lower pHRR and MARHE values, along with higher residual mass, indicating improved fire performance. Conversely, the APP–based systems show elevated

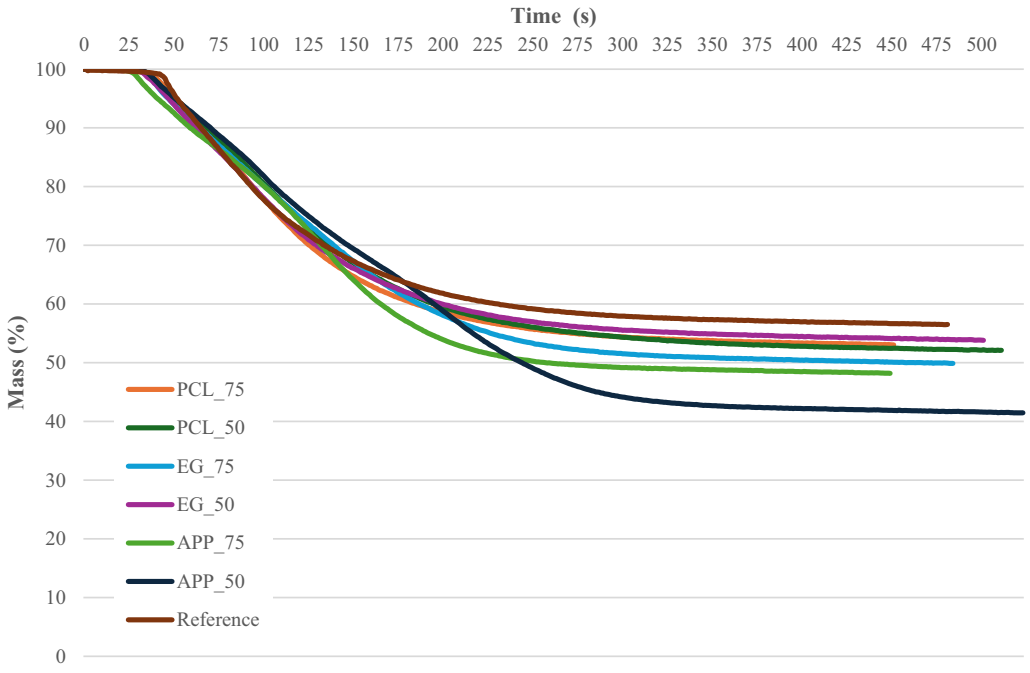

FIGURE 9 | Mass of composite specimens containing flame-retardant interlayers.

15480585, 2026, 4, Downloaded from https://4spepublications.onlinelibrary.wiley.com/doi/10.1002/vnl.70126 by Budapest University of Technology and Economics, Wiley Online Library on [02/08/2026]. See the Terms and Conditions (https://onlinelibrary.wiley.com/terms-and-conditions) on Wiley Online Library for rules of use; OA articles are governed by the applicable Creative Commons License

pHRR values and increased mass loss, reflecting the limited effectiveness of the protective layer in the investigated configuration.

Overall, the results demonstrate that, within the applied composite and interlayer configuration, EG provides better fire performance than APP. The reduced performance of flame retardants via PCL interlayers in CFRP composites compared to the neat PCL matrix arises because an additional, highly combustible thermoplastic layer is introduced into the carbon fiber-reinforced, crosslinked epoxy resin composite. Under cone calorimetry conditions, this PCL layer rapidly melts and can flow out of the sample edges, leading to ignition. In continuous composites, where the PCL cannot flow out, performance closer to that of the PCL matrix is expected.

3.2 | Structural Properties

3.2.1 | Tensile Test

First, tensile tests were carried out to investigate the effects of the applied flame-retardant additives on the mechanical properties of PCL. Tensile tests were conducted up to 50% strain. No failure of the tested specimens was observed within the investigated strain range. Characteristic tensile curves for each specimen type are shown in Figure 10. Tensile strength, strain at tensile strength, and tensile modulus of elasticity were determined from the measured data. The results are summarized in Table 7.

As Figure 10 and Table 7 demonstrate, both the use of APP and EG resulted in a significant improvement in tensile modulus and tensile strength compared to raw PCL. The addition of APP enhanced the tensile strength by more than 25% and the tensile modulus by ~45%. Meanwhile, in the case of EG, a ~45% increase in tensile strength and a more than 70% increase in tensile modulus was observed. Furthermore, the addition of the flame-retardants increased the strain at tensile strength value and resulted in an extended length of the plateau in the stress–strain curve in the region of the tensile strength.

3.2.2 | Flexural Test

Flexural tests were also carried out to investigate the influence of APP and EG on the mechanical properties of PCL. We did not experience any failure of the specimens during the tests. Therefore, the flexural tests were evaluated up to the conventional deflection, which equals 1.5 times the (nominal) thickness of the specimen corresponding to 3.5% flexural strain. Figure 11 shows flexural curves characteristic of each specimen type. From the measured data, flexural modulus and flexural stress at conventional deflection were determined (Table 7).

As Figure 11 and Table 7 show, similarly to the tensile tests, under bending load the application of the flame-retardants improved the mechanical properties significantly. Both APP and EG enhanced the flexural modulus and the flexural stress at conventional deflection by more than 38% compared to raw PCL. However, in contrast to the tensile tests, no statistically significant difference ($p > 0.05$) was observed between the effects of the two additives on the flexural properties.

The results of the quasi-static tensile and flexural tests indicate that the incorporation of EG or APP into the PCL matrix leads to increased modulus and strength of the material, which may be attributed to restricted polymer chain mobility and more efficient stress transfer in the presence of the rigid additives.

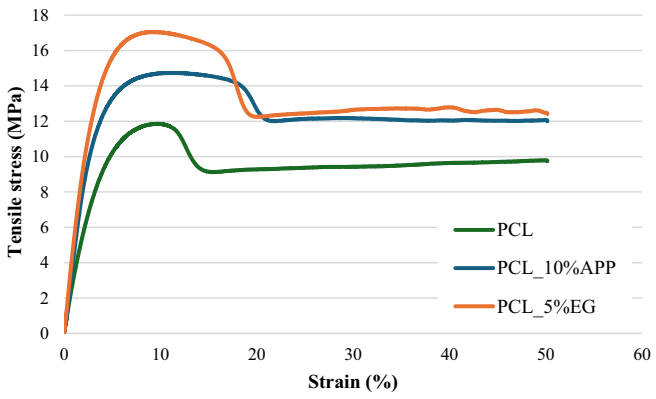

FIGURE 10 | Tensile curves characteristic to each specimen type.

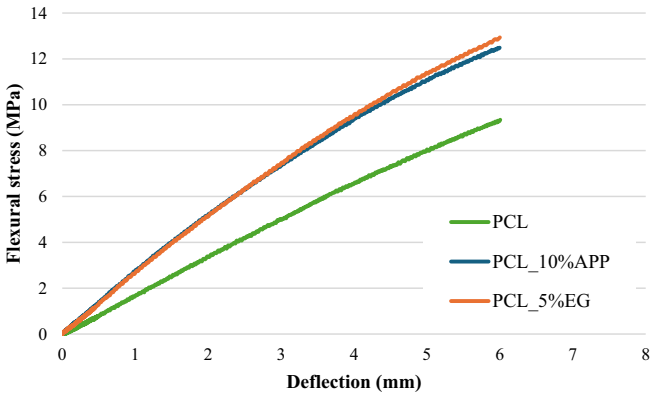

FIGURE 11 | Tensile curves characteristic to each specimen type.

TABLE 7 | Mean mechanical properties of the tested specimens (CoV in % expressed in brackets next to the sample mean values).

Sample	Tensile strength (MPa)	Tensile modulus (MPa)	Strain at strength (MPa)	Flexural modulus (MPa)	Flexural stress at conventional deflection (MPa)	Tensile impact strength (kJ/m²)
PCL	11.7 (4.6)	251.4 (8.9)	8.769 (10.889)	315.8 (9.1)	9.5 (4.1)	249.8 (7.5)
PCL_10%APP	14.9 (6.3)	364.7 (18.3)	11.105 (6.107)	437.4 (2.0)	13.1 (2.0)	189.2 (8.1)
PCL_5%EG	17.1 (2.6)	435.9 (10.2)	9.436 (3.41)	439.3 (4.4)	13.4 (3.3)	46.0 (5.5)

15480585, 2026, 4, Downloaded from https://4spepublications.onlinelibrary.wiley.com/doi/10.1002/vnl.70126 by Budapest University of Technology and Economics, Wiley Online Library on [02/08/2026]. See the Terms and Conditions (https://onlinelibrary.wiley.com/terms-and-conditions) on Wiley Online Library for rules of use; OA articles are governed by the applicable Creative Commons License

3.2.3 | Tensile Impact Tests

Besides quasi-static tensile and flexural tests, tensile impact tests were conducted to evaluate the effects of the flame-retardants on the behavior of PCL under impact load. The results of the experiments are summarized in Table 7.

The results in Table 7 indicate that the incorporation of the rigid particles as additives results in a more brittle behavior, thereby in a decrease in the tensile impact strength compared to the ductile raw PCL material. However, we experienced a significant difference between the effects of the two types of additives. Meanwhile, the use of APP reduced the tensile impact strength by less than 25%; in the case of EG, a more than 80% decrease was observed.

This phenomenon may be explained as attributed to differences in particle geometry. While the plate-like morphology of EG promotes severe stress concentrations and premature crack initiation, particularly under dynamic loading, the more spherical particulate geometry of APP results in less pronounced stress localization.

The enhancement in tensile and flexural performance is likely governed by the combined effect of the incorporated additives acting both as reinforcing phase and nucleating agents. The presence of EG and APP introduces rigid inclusions into the matrix, limiting chain mobility and contributing to increased stiffness. In addition, the shift of the crystallization temperature observed in DSC measurements indicates intensified heterogeneous nucleation, which promotes a higher crystalline fraction and improves load transfer efficiency in the semi-crystalline structure. It should also be noted that the mechanical response of such systems strongly depends on the dispersion quality of the additives, as a uniform distribution can lead to reinforcement while particle agglomeration may act as defect sites and reduce mechanical performance [25].

4 | Conclusions

In this study, flame-retardant PCL filaments were developed and applied as additively manufactured interlayers in carbon-fiber reinforced epoxy resin composites. The aim was to evaluate how 5 mass% EG and 10 mass% APP affect the crystallization, mechanical properties, and fire behavior of PCL, and how these effects translate to composite laminates when applied as flame retarded interlayers. The work further addressed the feasibility of using additive manufacturing for the localized placement of multifunctional thermoplastic interlayers within fiber-reinforced composite structures.

Thermal analysis showed that EG and APP increased the PCL crystallization peak from 22.96°C (neat PCL) to 40.80°C and 34.12°C, respectively, demonstrating strong nucleating effects. EG increased the quasi-static tensile modulus by more than 70% without reducing elongation at break, whereas APP also increased the modulus to a lesser extent (~45%) and only slightly reduced ductility. The simultaneous improvement in stiffness and strength is attributed to the combined reinforcing and heterogeneous nucleating action of the flame-retardant additives, which restrict polymer chain mobility while promoting more efficient stress transfer within the crystalline structure. Cone calorimetry revealed a 25% reduction in peak heat release rate (pHRR) for EG-modified PCL.

When used as interlayers in CFRP laminates, the flame-retardant effect was less pronounced (pHRR decreased from 346 to 311 kW/m^2) because an additional, highly combustible thermoplastic layer is introduced into the crosslinked, carbon-fiber-rich composite. Under cone calorimetry conditions, this PCL layer rapidly melts and can flow out of the sample edges, leading to ignition. This behavior highlights a key design limitation of localized thermoplastic interlayers, where melt flow can hinder the formation of a continuous protective barrier despite the presence of flame retardants. In continuous composites, where PCL cannot flow, performance closer to that of the neat PCL matrix is expected. The relatively moderate fire-retardant effect observed is also related to the low additive loadings required to maintain filament printability and extrusion stability, indicating that optimization of additive concentration, synergistic systems, and interlayer geometry represents an important direction for future work.

Rather than acting as a bulk flame-retardant solution, the interlayer concept represents a strategy for combining damage tolerance enhancement with local fire-safety functionality. The successful implementation of additively manufactured flame-retarded PCL interlayers therefore supports the development of next-generation composite systems in which mechanical performance, failure behavior, and fire response can be tailored simultaneously through architectured interlayer design.

Author Contributions

Andrea Toldy: conceptualization, funding acquisition, writing – original draft, writing – review and editing, project administration, supervision, resources, methodology, visualization. **Gergő Zsolt Marton:** investigation, writing – original draft, writing – review and editing, methodology. **Gábor Szebényi:** conceptualization, funding acquisition, writing – original draft, writing – review and editing, project administration, resources, supervision. **László József Varga:** investigation, methodology. **Fanni Balogh:** conceptualization, investigation, writing – original draft, writing – review and editing, visualization, methodology, validation.

Acknowledgments

This research was funded by the National Research, Development and Innovation Office (NKFIH K142517 and FK 142540). Project no. KDP-IKT-2023-900-I1-00000957/0000003 has been implemented with the support provided by the Ministry of Culture and Innovation of Hungary from the National Research, Development and Innovation Fund, financed under the KDP-2023 funding scheme. The project supported by the Doctoral Excellence Fellowship Programme (DCEP) is funded by the National Research Development and Innovation Fund of the Ministry of Culture and Innovation and the Budapest University of Technology and Economics. Special thanks to Noémi Bocsó for her help with the experiments. Gábor Szebényi acknowledges the financial support received through the János Bolyai Scholarship of the Hungarian Academy of Sciences. 2022-2.1.1-NL-2022-00012 "National Laboratory for Cooperative Technologies" has been implemented with the support provided by the Ministry of Culture and Innovation of Hungary from the National Research, Development and Innovation Fund, financed under the National Laboratories funding scheme.

15480585, 2026, 4, Downloaded from https://4spepublications.onlinelibrary.wiley.com/doi/10.1002/vnl.70126 by Budapest University of Technology and Economics, Wiley Online Library on [02/08/2026]. See the Terms and Conditions (https://onlinelibrary.wiley.com/terms-and-conditions) on Wiley Online Library for rules of use; OA articles are governed by the applicable Creative Commons License

During the preparation of this work the authors used ChatGPT and Grammarly in order to improve the language and readability of the paper. After using this tool, the author(s) reviewed and edited the content as needed and take full responsibility for the content of the published article.

Funding

This research was funded by the National Research, Development and Innovation Office (NKFIH K142517 and FK 142540). Project no. KDP-IKT-2023-900-I1-00000957/0000003 has been implemented with the support provided by the Ministry of Culture and Innovation of Hungary from the National Research, Development and Innovation Fund, financed under the KDP-2023 funding scheme. The project supported by the Doctoral Excellence Fellowship Programme (DCEP) is funded by the National Research Development and Innovation Fund of the Ministry of Culture and Innovation and the Budapest University of Technology and Economics. Gábor Szebényi acknowledges the financial support received through the János Bolyai Scholarship of the Hungarian Academy of Sciences. 2022-2.1.1-NL-2022-00012 "National Laboratory for Cooperative Technologies" has been implemented with the support provided by the Ministry of Culture and Innovation of Hungary from the National Research, Development and Innovation Fund, financed under the National Laboratories funding scheme.

Conflicts of Interest

The authors declare no conflicts of interest.

Data Availability Statement

The data that support the findings of this study are available from the corresponding author upon reasonable request.

References

1. A. Toldy, B. Szolnoki, and M. Gy, "Flame Retardancy of Fibre-Reinforced Epoxy Resin Composites for Aerospace Applications," *Polymer Degradation and Stability* 96, no. 3 (2011): 371–376, https://doi.org/10.1016/j.polymdegradstab.2010.03.021.

2. A. Toldy, "Safe and Sustainable-By-Design: Redefining Polymer Engineering for a Greener Future," *Express Polymer Letters* 19, no. 4 (2025): 350, https://doi.org/10.3144/expresspolymlett.2025.25.

3. A. K. Hamzat, M. S. Murad, I. A. Adediran, E. Asmatulu, and R. Asmatulu, "Fiber-Reinforced Composites for Aerospace, Energy, and Marine Applications: An Insight Into Failure Mechanisms Under Chemical, Thermal, Oxidative, and Mechanical Load Conditions," *Advanced Composites and Hybrid Materials* 8, no. 1 (2025): 152, https://doi.org/10.1007/s42114-024-01192-y.

4. G. Z. Marton and G. Szebényi, "Influencing the Damage Process and Failure Behaviour of Polymer Composites—A Short Review," *Express Polymer Letters* 19, no. 2 (2025): 140–160, https://doi.org/10.3144/expresspolymlett.2025.11.

5. B. Magyar, T. Czigány, and G. Szebényi, "Metal-Alike Polymer Composites: The Effect of Inter-Layer Content on the Pseudo-Ductile Behaviour of Carbon Fibre/Epoxy Resin Materials," *Composites Science and Technology* 215 (2021): 109002, https://doi.org/10.1016/j.compscitech.2021.109002.

6. S. G. Marino and G. Czél, "Development and Characterisation of Reparable, Film Interleaved, Pseudo-Ductile Hybrid Composites," *Composites Part A: Applied Science and Manufacturing* 169 (2023): 107496, https://doi.org/10.1016/j.compositesa.2023.107496.

7. L. McKeen, "The Effect of Heat Aging on the Properties of Polyesters," in *The Effect of Long Term Thermal Exposure on Plastics and Elastomers* (William Andrew Publishing, 2021), 83–116, https://doi.org/10.1016/b978-0-323-85436-8.00003-5.

8. X. Y. Zhang, X. Peng, and S. N. Zhang, *Synthetic Biodegradable Medical Polymers*, vol. 1 (Elsevier, 2017), 217–254, https://doi.org/10.1016/b978-0-08-100372-5.00007-6.

9. L. Jiang and J. Zhang, *Biodegradable Polymers and Polymer Blends* (Elsevier, 2012), 109–128, https://doi.org/10.1016/b978-1-4557-2834-3.00006-9.

10. K. Deshmukh, M. B. Ahamed, R. R. Deshmukh, S. K. K. Pasha, P. R. Bhagat, and K. Chidambaram, *Biopolymer Composites With High Dielectric Performance: Interface Engineering* (Elsevier, 2016), 27–128, https://doi.org/10.1016/b978-0-12-809261-3.00003-6.

11. S. K. Siddhamalli, "Toughening of Epoxy/Polycaprolactone Composites via Reaction Induced Phase Separation," *Polymer Composites* 21, no. 5 (2000): 846–855, https://doi.org/10.1002/pc.10239.

12. G. Szebenyi, T. Czigany, B. Magyar, and J. Karger-Kocsis, "3D Printing-Assisted Interphase Engineering of Polymer Composites: Concept and Feasibility," *Express Polymer Letters* 11, no. 7 (2017): 525–530, https://doi.org/10.3144/expresspolymlett.2017.50.

13. G. Szebényi, B. Magyar, and T. Czigany, "Achieving Pseudo-Ductile Behavior of Carbon Fiber Reinforced Polymer Composites via Interfacial Engineering," *Advanced Engineering Materials* 23, no. 2 (2020): 2000822, https://doi.org/10.1002/adem.202000822.

14. G. Z. Marton, Á. Fendrik, and G. Szebényi, "Manufacturing of Composites With Designed Failure," *IOP Conference Series: Materials Science and Engineering* 1313, no. 1 (2024): 012014, https://doi.org/10.1088/1757-899x/1313/1/012014.

15. M. R. Carotenuto, G. Cavallaro, I. Chinnici, G. Lazzara, and S. Milioto, "Thermomechanical Properties of Bionanocomposites Based on Polycaprolactone and Halloysite Clay Nanotubes," *Journal of Thermal Analysis and Calorimetry* 150, no. 10 (2025): 7519–7528, https://doi.org/10.1007/s10973-025-14178-9.

16. S. F. Hansen, F. Paulsen, and X. Trier, "Smart Materials and Safe and Sustainable-By-Design: A Feasibility and Policy Analysis," in *Ensuring the Environmental Sustainability of Emerging Technologies*, ed. M. V. Florin (EPFL International Risk Governance Center, 2023), https://doi.org/10.5075/epfl-irgc-298445.

17. H. Wu, M. Sulkis, J. Driver, A. Saade-Castillo, A. Thompson, and J. H. Koo, "Multi-Functional ULTEM1010 Composite Filaments for Additive Manufacturing Using Fused Filament Fabrication (FFF)," *Additive Manufacturing* 24 (2018): 298–306, https://doi.org/10.1016/j.addma.2018.10.014.

18. W. Tabaka, D. Meinel, and B. Schartel, "Sacrifice Few to Save Many: Fire Protective Interlayers in Carbon-Fiber-Reinforced Laminates," *ACS Omega* 9, no. 22 (2024): 23703–23712, https://doi.org/10.1021/acsomega.4c01408.

19. Z. Wang, T. Yan, Y. Gao, X. Ma, P. Xu, and Y. Ding, "Improving Flame Retardant and Electromagnetic Interference Shielding Properties of Poly(Lactic Acid)/poly(ε-Caprolactone) Composites Using Catalytic Imidazolium Modified CNTs and Ammonium Polyphosphate," *International Journal of Biological Macromolecules* 259, no. Pt 2 (2024): 129265, https://doi.org/10.1016/j.ijbiomac.2024.129265.

20. Y. Chen, Z. Zhou, Y. Chen, Q. Yuan, W. Zhang, and J. Huang, "Enhancing Fire-Resistant Performance and Mechanical Property of PLA/PCL Composite Films by the Synergistic Effect of BC–NPA and MXene," *Industrial Crops and Products* 232 (2025): 121323, https://doi.org/10.1016/j.indcrop.2025.121323.

21. J. Aqil Ahmed and P. Amuthakkannan, "Thermal Characterisation and Flame Retardancy Enhancement of PLA, PCL & Hybrid Composites Using Sustainable Marble Powder Filler," *Materials*

15480585, 2026, 4, Downloaded from https://4spepublications.onlinelibrary.wiley.com/doi/10.1002/vnl.70126 by Budapest University of Technology and Economics, Wiley Online Library on [02/08/2026]. See the Terms and Conditions (https://onlinelibrary.wiley.com/terms-and-conditions) on Wiley Online Library for rules of use; OA articles are governed by the applicable Creative Commons License

Research Express 12, no. 8 (2025): 085303, https://doi.org/10.1088/2053-1591/adf70d.

22. K. Babu, O. Das, V. Shanmugam, et al., "Fire Behavior of 3D-Printed Polymeric Composites," *Journal of Materials Engineering and Performance* 30, no. 7 (2021): 4745–4755, https://doi.org/10.1007/s11665-021-05627-1.

23. M. A. Ntrivala, A. C. Pitsavas, K. Lazaridou, et al., "Polycaprolactone (PCL): The Biodegradable Polyester Shaping the Future of Materials – A Review on Synthesis, Properties, Biodegradation, Applications and Future Perspectives," *European Polymer Journal* 234 (2025): 114033, https://doi.org/10.1016/j.eurpolymj.2025.114033.

24. V. Crescenzi, G. Manzini, G. Calzolari, and C. Borri, "Thermodynamics of Fusion of Poly-β-Propiolactone and Poly-ε-Caprolactone. Comparative Analysis of the Melting of Aliphatic Polylactone and Polyester Chains," *European Polymer Journal* 8, no. 3 (1972): 449–463, https://doi.org/10.1016/0014-3057(72)90109-7.

25. A. Toldy, D. I. Poór, B. Szolnoki, N. Geier, and Á. Pomázi, "Synergistic Flame Retardancy of Carbon Fibre-Reinforced Polyimine Vitrimer Composites via Vitrimer-Based Intumescent Coating," *Composites Part A Applied Science and Manufacturing* 198 (2025): 109135, https://doi.org/10.1016/j.compositesa.2025.109135.

15480585, 2026, 4, Downloaded from https://4spepublications.onlinelibrary.wiley.com/doi/10.1002/vnl.70126 by Budapest University of Technology and Economics, Wiley Online Library on [02/08/2026]. See the Terms and Conditions (https://onlinelibrary.wiley.com/terms-and-conditions) on Wiley Online Library for rules of use; OA articles are governed by the applicable Creative Commons License